Talanta 129 (2014) 276–281

Contents lists available at ScienceDirect

Talanta

journal homepage: www.elsevier.com/locate/talanta

Glucose biosensor based on multisegment nanowires exhibiting reversible magnetic control

Gislaine P. Gerola, Giovanna S. Takahashi, Geraldo G. Perez, Lucas C. Recco, Valber A. Pedrosa*

Institute of Bioscience, Department of Chemistry and Biochemistry, UNESP, Botucatu-SP, Brazil

ARTICLE INFO

Article history:
Received 21 March 2014
Received in revised form
18 May 2014
Accepted 19 May 2014
Available online 4 June 2014

Keywords:
Biosensor
Nanowires orientation
Reversible modulation

ABSTRACT

We describe the amperometric detection of glucose using oriented nanowires with magnetic switching of the bioelectrochemical process. The fabrication process of the nanowires was prepared through controlled nucleation and growth during a stepwise electrochemical deposition, and it was characterized using scanning electron microscopy. Cyclic voltammetry and amperometry were used to study the magnetoswitchable property; this control was accomplished by changing the surface orientation of nanowires. Under the optimal condition, the amperometric response was also linear up to a glucose concentration of 0.1–16.0 mmol L^{-1} with a sensitivity of 81 μA mM^{-1}. The detection limit was estimated for 4.8×10^{-8} mol L^{-1}, defined from a signal/noise ratio of 3. It also exhibits good reproducibility and high selectivity with insignificant interference from ascorbic acid, acetoaminophen, and uric acid. The resulting biosensor was applied to detect the blood sugar in human serum samples without any pretreatment, and the results were comparatively in agreement with the clinical assay.

1. Introduction

There is still great interest in the development of biosensors with high sensitivity, low cost, and reliability for a variety of biological and biomedical application [1–4]. Nanostructured materials have received increasing interest because of their promise of fast, accurate, and inexpensive ways to measure an extremely wide variety of analytes produced or consumed in biological and biochemical processes and also measure more directly the activity of biological systems or their components [5–7]. The combination of nanometer materials and biomolecules is of interest in the field of biosensor development because nanostructures can play an important role in immobilization of biomolecules because of their large specific surface area, excellent biocompatibility, and good conductivity. Nanomaterials have improved the electron transfer rate between enzyme and electrode surface. Because of the favorable electrocatalytic effect and large specific surface area, nanomaterials can immobilize protein macromolecules [8–9] and enhance the enzyme absorption and facilitate electron transfer between the immobilized proteins and the surface of electrodes [10–11]. These properties have led to the use of nanomaterials for the development of biosensors to enhance analytical performance [12–13].

Nanowires are more attractive in recent years because of their versatile roles in bioelectronic applications and excellent properties of responding to chemical [14], optical [15], or magnetic [16] external signals controlling the activity of the systems. For example, Liu et al. fabricated ZnO nanowire-based biologically sensitive field-effect transistors for the detection of different concentrations of uric acid solution [17]. Wang et al. successfully reported a glucose sensor by the chemical cross-linking method with glutaraldehyde in the presence of gold nanowires [18]. Ibupoto et al. constructed a sensitive method to detect C-reactive protein using ZnO nanomaterial [19]. Wang et al. reported an attractive strategy to build biosensor with aligned surface controlled by magnetic property [20]. They reported the application of nanowires for magnetic control of the electrochemical reactivity to demonstrate how one can modulate the electrocatalytic activity by orienting catalytic nanowires at different angles. Unlike early "on/off" magnetic switching studies based on functionalized magnetic spheres, the present magnetoswitchable protocol relies on modulating the electrochemical reactivity without removing the magnetic material from the surface. The nanowire-based magnetoswitchable protocol may be extremely useful for adjusting the electrochemical reactivity, such as external control of catalytic transformations in bioreactors [21], tailoring of reversible amperometric immunosensors [22], regeneration of enzyme-biosensor electrodes [23], and external triggering of biofuel cells [24].

We describe a biosensor based on multisegment nanowires with magnetic properties. The immobilization of glucose oxidase on the nanowires was derivatized with EDC/NHS as the cross-linking agent.

* Corresponding author. Tel.: +55 14 38800576.
E-mail address: vpedrosa@ibb.unesp.br (V.A. Pedrosa).

http://dx.doi.org/10.1016/j.talanta.2014.05.035
0039-9140/

The electrochemical performance of the biosensor was investigated using cyclic voltammetry and amperometry. The effect of pH, applied potential, and amount of enzymes were also evaluated. The biosensor showed an excellent performance for the detection of glucose with high selectivity and reproducibility. The developed device could open the door to a wide range of novel electrocatalytic and bioelectrocatalytic applications of magneto-controlled redox enzymes. Furthermore, it could be used in miniaturized and portable biosensing systems, such as lab-on-a-chip devices, in medical and environmental applications that have a restricted quantity of samples.

2. Experimental

2.1. Reagents and materials

Pyrrole (PPy), glucose oxidase (EC 1.1.3.4, 235 unit mg^{-1}), 3-mercaptopropionic acid (3-MPA), ethyl(dimethylaminopropyl) carbodiimide (EDC), N-hydroxysulfosuccinimide (NHS), glucose, phosphate buffer (PBS), $CuSO_4 \cdot 5H_2O$, $NiCl_2 \cdot 6H_2O$–$Ni(H_2NSO_3)_2 \cdot 4H_2O$–$H_3BO_3$, Ag_2SO_4, KSCN, H_3BO_3, ferrocene monocarboxylic acid (FMCA) were obtained from Sigma-Aldrich. Anodisc alumina membranes, with a pore size of 200 nm and thickness of 60 μm, were purchased from Whatman (Maidstone, U.K.). Ultrapure water (18.2 MΩ cm) from the Milli-Q (Millipore Inc. USA) purification system was used in all of the experiments.

2.2. Apparatus

The electrochemical measurements were conducted in a three electrode Pyrex® cell. All controlled-potential experiments were performed with the μAutolab Type III/FRA2 response analyzer (Eco Chemie BV). Glass carbon electrode was used as working electrode, platinum wire served as the counter electrode, while Ag/AgCl served as the reference electrode. Cyclic voltammograms were recorded in the presence of 0.5 mM FMCA. Chronoamperometry was used to characterize response of electrochemical biosensors to glucose. Glucose aliquots of known concentration were added into the electrochemical cell after the background current stabilized. SEM images were taken with a Quanta 200 (FEI company) field-emission scanning electron microscope operating at an acceleration voltage of 20 kV.

2.3. Synthesis and modification of nickel/pyrrole-GOx nanowires

The nanowires were prepared electrochemically using a membrane-template synthesis method [25]. The desired length of the segment was electrodeposited into the nanopores of the alumina membrane template by controlling the electrodeposition charge. A gold film was first sputtered on one side of the template to serve as a working electrode. The membrane was assembled in a plating cell with aluminum foil serving as a contact for the sputtered gold. An initial copper layer was first electrodeposited from a 1 mol L^{-1} $CuSO_4 \cdot 5H_2O$ solution applying 5 C (C) at −1.0 V (vs. Ag/AgCl in connection to a Pt wire counter electrode). Then gold was plated (10 C) at −0.9 V from the commercial gold plating solution. After the gold segment, silver was deposited (5 C) from a 0.05 mol L^{-1} Ag_2SO_4+2.3 mol L^{-1} KSCN solution (pH=6.0), at room temperature. Subsequently PPy was deposited. The electropolymerization solution consisted of 0.5 mol L^{-1} pyrrole and 0.1% v/v Tween 20 in deionized water (without added electrolyte). The electropolymerization proceeded potentiostatically (at +0.8 V), until the desired amount of charge was passed. Subsequently, nickel (10 C) was electrodeposited at −1.0 V from a solution containing 20 g L^{-1} $NiCl_2 \cdot 6H_2O$, 515 g L^{-1} $Ni(H_2NSO_3)_2 \cdot 4H_2O$, and 20 g $L^{-1}H_3BO_3$ (buffered to pH 3.4).

After depositing the nanowires, the sputtered gold layer was removed by mechanical polishing using cotton tips. The nanowires were then removed from the template by dissolving the alumina in an agitated 3 mol L^{-1} NaOH solution for 30 min. The resulting Au/Ag/PPY/Ni nanowires were washed repeatedly with water to remove the residual base and salt. A small magnet was placed to collect the nanowires on a sidewall of a glass vial and the water was decanted.

Immediately after the cleaning step, the nanowires were modified by immersion in a 1.0×10^{-3} mol L^{-1} 3-MPA ethanolic solution for 2 h. The electrode was immersed in 5 mL of phosphate buffer solution (10 mmol L^{-1}, pH 5.5) containing 0.4 mol L^{-1} EDC and 0.1 mol L^{-1} NHS for about 2 h with continuous stirring for activation of the −COOH group, then added to 100 μL GOx (10 mg mL^{-1} in 10 mmol L^{-1} of PBS at pH 6.0) and stirred overnight.

2.4. Measurement procedure

Prior to use, the surface of the glassy carbon electrode was thoroughly polished with 3.0 and 0.05 μm alumina slurries and rinsed with deionized water. Anodic stripping voltammetric measurements were performed either at the bare glassy carbon (GC) covered with the nanowires (held by an external magnetic field). The orientation of the functionalized nanowires was switched by rotating an external magnet (placed under the working electrode) for 90°. The nanowires were aligned in the “vertical” position with respect to the surface during the “active” state and were switched to the “horizontal” position for the “passive” state (between the measurements). Analytical curves were obtained by the standard addition method. In interferent experiments, 0.5 mM of ascorbic acid, uric acid and acetoaminophen were used instead of glucose, under conditions identical. Each experiment was repeated three times, and the reported error corresponds to the standard deviation of the measured values. All the reactions were performed at open atmosphere and ambient temperature without a solution purge of oxygen.

Serum samples were provided by a local hospital, which were analyzed with Boehringer enzyme kit by spectrophotometric. The analytical procedure was performed according to the manufacturer's manual. The biosensor was applied to glucose determination in several serum samples. The blood samples were centrifuged at 4000 r/m for 5 min at room temperature to separate the serum. All the samples were submitted to the above processes and each test was performed in triplicate.

3. Results and discussion

3.1. Preparation and characterization of the nanowires.

Fig. 1A shows cyclic voltammograms of FMCA, horizontal orientation, that redox reaction easily occurred well-defined electrochemical response of the soluble redox species confirms the electrode ON state due to contact of the enzyme and the surface-bound mediator. Switching the nanowires to the vertical position of the CV curves shows a decrease of current for both anodic and cathodic processes, confirming that the biosensor is in off state and reduces the electron-transfer processes of the redox probe in the solution [26]. Also, SEM was used to monitor the procedure of nanowires. Fig. 1B shows the SEM image of the Au/Ag/PPy/Ni, revealing a smooth surface and an average diameter of 20 nm. As observed from Fig. 1B, well-ordered Au/Ag/PPy/Ni nanowires were synthesized. In the cross-section image, the average length of nanowires was estimated to be about 6 μm.

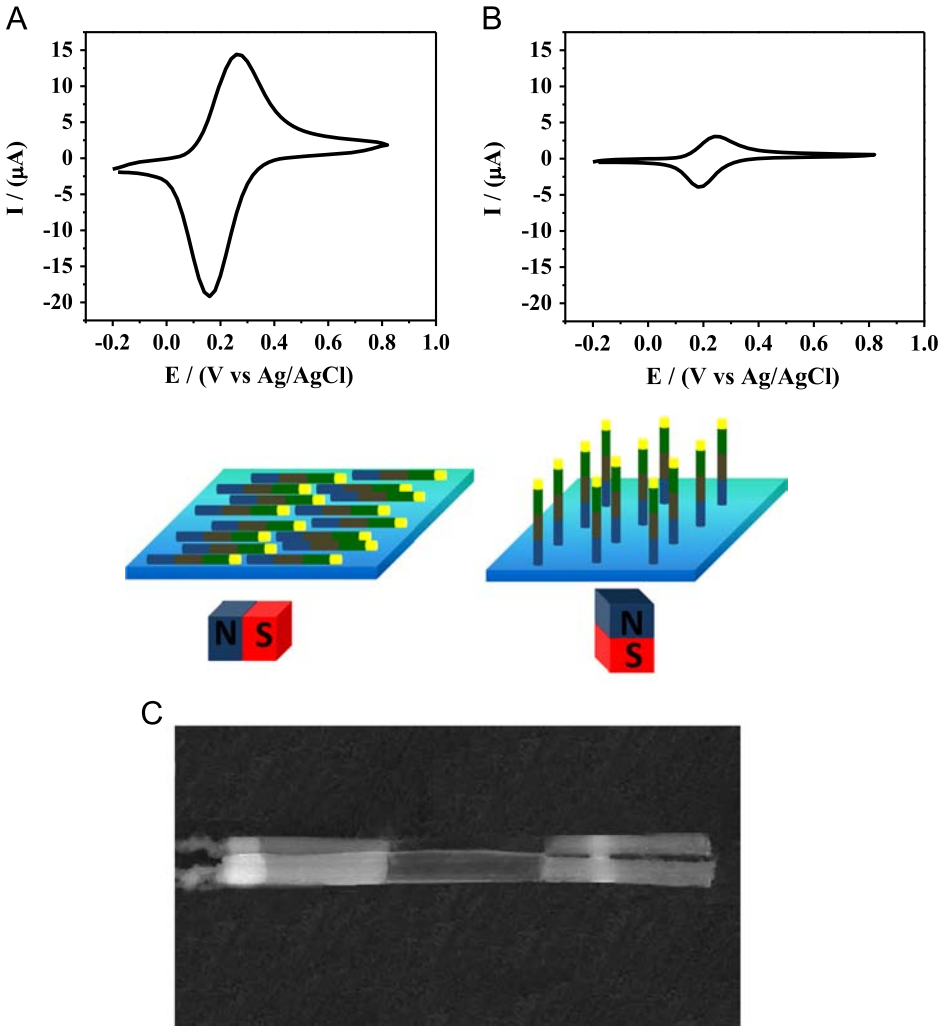

Fig. 1. Cyclic voltammograms obtained with the magnetic field oriented of the nanowires in the horizontal (A) and vertical (B) positions, in the presence of 0.5 mmol L^{-1} FMCA + 10 mmol L^{-1} PBS (pH = 6.0). (C) SEM image of the synthesized Au/Ag/PPy/Ni nanowires.

3.2. Electrochemical performance of the nanowires

The ability to use nanowires for magnetic control of electrochemical processes is illustrated in Fig. 2 in connection to electrocatalytic measurements of glucose. Fig. 2 shows the amperometric response for glucose in the presence of nanowires magnetically oriented in the vertical (a) and horizontal (b) positions. Positioning the nanowires on the surface of the thick-film carbon electrode, with the magnetic field in the vertical orientation, leads to a dramatic enhancement of the signal (a), reflecting the catalytic action of the nanowires. A substantial decrease of this response is observed upon switching the magnetic field and, in turn, the nanowires from the vertical to the horizontal position (b). Such magnetically modulated redox transformations can be repeated multiple times upon repetitive changes of the surface orientation. The corresponding signal changes are highly reproducible and fast. Following five reorientation cycles, the magnetic field was removed, retracting the nanowires from the surface and returning the response to its background value. Such magnetic modulation of electrochemical transformations reflects changes in the accessibility of the glucose to the nickel catalytic sites upon switching between the two surface orientations. Although the catalytic sites are fully accessible to the solute in the vertical orientation, switching to the horizontal position partially "blocks" them, hindering the solute transport to the portion of the nickel surface facing the carbon support. Such surface effects are opposite to what is expected because of magneto hydrodynamic effects, which are pronounced when the magnetic field is parallel to the electrode surface (i.e., when the nanowires are in the horizontal position) and negligible when perpendicular.

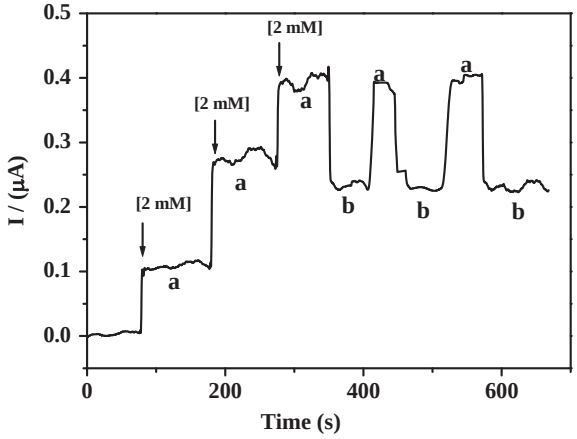

Fig. 2. Amperometric response for 2 mmol L^{-1} glucose, with the nanowires oriented in the vertical (a) and horizontal (b) positions. Applied potential +0.4 V (vs. Ag/AgCl) in 0.5 mmol L^{-1} FMCA + 10 mmol L^{-1} M PBS (pH = 6.0).

To test such behavior, the electrochemical response of nanowires deposited onto electrode was examined with chronoamperometric

experiments, which can also provide valuable insights of the diffusion coefficient. The Cottrell equation (1) describes the evolution of the current with the respect to time in a controlled potential experiment [27]

$$i = nFAD^{1/2}c/\pi^{1/2}t^{1/2} \quad (1)$$

where n is the number of electrons involved in the process, F is the Faraday constant, A is the area of the electrode, C is the bulk concentration, D is the diffusion coefficient for species, and t is the time. Fig. 3 shows Cottrell plots for FMCA oxidation at glass carbon electrode with the nanowires from the horizontal (1) to the vertical (2) position. With the nanowires in the vertical position, the anodic current transient decays within ~200 ms. For comparison, the current transient in horizontal position decays substantially slower—within ~350 ms, which indicates faster electron transfer in the vertical position. These results indicate that the diffusional barrier imposed by the horizontal position should also be considered because it influences biosensor response. From Eq. (1), D was calculated as 5.4×10^{-7} cm^2 s^{-1}. A semi-linear relation was found in the plot I vs. $t^{-1/2}$ in the region 1.0–3.5 s (inset), which confirms that D is strongly dependent on mass transport. This suggests that mass transport and diffusion are partially blocked at the horizontal position and may partly explain the decrease of current shown in Fig. 2.

3.3. Optimization of biosensor

Fig. 4A shows a study of the influence of the amount of enzyme added to the electrode on the current response measured as a consequence of the anodic oxidation of FMCA. Experiments were carried out in a 0.5 mmol L^{-1} FMCA solution prepared in 10 mmol L^{-1} PBS. The amount of enzyme immobilized onto the nanowires varied between 0.1 and 0.6 mg mL^{-1}. Analysis of the results shows that the current increases linearly up to 0.4 mg mL^{-1}, which is an indication that the enzymatic reaction is the rate-controlling step. By increasing the amount of immobilized enzyme, no further current increase is observed because mass transport becomes the rate-determining step. The mass-transfer controlling ion is preferred for an enzyme electrode as the response becomes relatively insensitive to slight changes in enzyme activity; hence, the biosensor operational and storage lifetime is extended. Also, we tested the dependence of the biosensor response on the pH of 6.0–9.0 in phosphate buffers containing 0.5 mmol L^{-1} FMCA as shown in Fig. 4B. The peak potential related to the oxidation of FMCA was found to be strongly affected by the pH, with I_{pa} varying

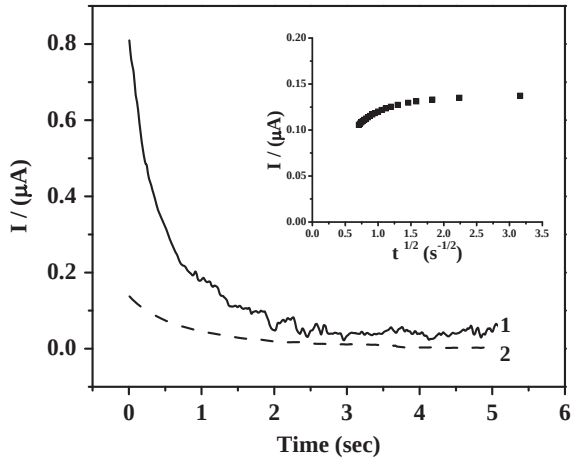

Fig. 3. The chronoamperometric responses of the nanowires oriented in the vertical (1) and horizontal (2) positions in 10 mmol L^{-1} PBS at potential step of 0.3 V. The inset shows the plot of I vs. $t^{-1/2}$ obtained from the chronoamperograms with nanowires in vertical position.

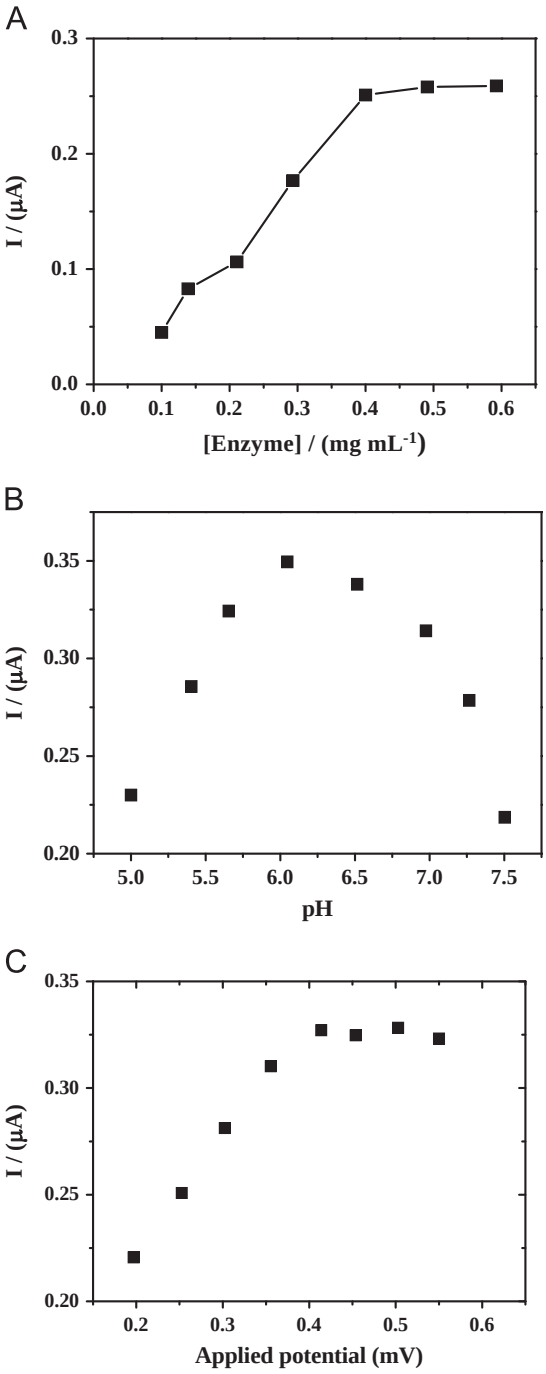

Fig. 4. (A) Effect of enzyme loading on the response of the biosensor in a 0.5 mmol L^{-1} FMCA 10 mmol L^{-1} PBS (pH 6.0). (B) Influence of the pH on peak current, and (C) the effect of potential dependence on the biosensor response to 0.5 mmol L^{-1} FMCA in 10 mmol L^{-1} PBS, pH=6.0.

from 0.22 to 0.35 μA as the pH is increased in the investigated range. Moreover, the I_p vs. pH plot revealed a maximum current at approximately pH 6.0, with I_p decreasing sharply in both directions. Hence, all subsequent experiments were carried out at pH 6.0. The applied potential is also an important parameter that affects the sensitivity of the modified sensor. As shown in Fig. 4C, the current response increased from 0.22 μA (at the potential of 0.2 V) up to the maximum value of 0.33 μA (at the potential of 0.4 V). Therefore, 0.4 V was chosen as the optimal applied potential to obtain a high sensitivity.

3.4. Analytical parameters

The bioelectrocatalysis oxidation of glucose was studied using amperometry at different concentrations of glucose. Fig. 5 shows a typical amperometric response at 0.4 V of the modified electrode to successive addition of glucose to stirred PBS, thus increasing the glucose concentration at 2.0 mmol L^{-1} per step. Immediately after the addition of glucose, the response increases and reaches a steady state within 10 s, indicating a good catalytic property of the biosensor. The calibration curve of the glucose concentration vs. current is shown in an inset upper of Fig. 5, which clearly reveals the linear relation between the current and glucose concentrations. The response displays a linear range of 2.0–16 mmol L^{-1} with a correlation coefficient of 0.989 and a slope of 81 μA mM^{-1}. The detection limit was estimated to be 4.8×10^{-8} mol L^{-1} at a signal/noise ratio (*S*/*N*) of 3. The repeatability is expressed as the relative standard deviation (RSD 5.2%) value of the current obtained for ten injections of the same concentration of glucose at different times. These results reveal that the biosensor has higher enzymatic activity with higher affinity to glucose. The present configuration of the biosensor shows lower detection and sensitivity, which is lower than some biosensors based on nanostructure configuration for glucose sensing [28–31].

3.5. Specificity to glucose in the presence of interfering substances

Small molecules, such as ascorbic acid (AA), acetoaminophen (AP), and uric acid (UA), are present in physiological fluids and can be oxidized at the electrode, thus masking sensor response to glucose or hydrogen peroxide. Common interference needs to be seriously considered because they could be oxidized at the same potential. We investigated the effects of 0.5 mmol L^{-1} AA, AP, and UA on the glucose sensor response at anodic potentials. Fig. 6A shows amperometric injection of AA, AP, and UA oxidation at the biosensor. Poising the electrode at 0.4 V and introducing 0.5 mmol L^{-1} AA, AP, and UA did not result in appreciable oxidation currents. In comparison, the addition of 0.5 mmol L^{-1} glucose produced a strong jump in the current, pointing to the breakdown of glucose by GOx. These results demonstrate that the biosensor was selective to glucose in the presence of other interfering substances.

3.6. Storage stability

Fig. 6b shows the sensor response for 2 mmol L^{-1} concentration of glucose recorded over a 30-day period. When the biosensor

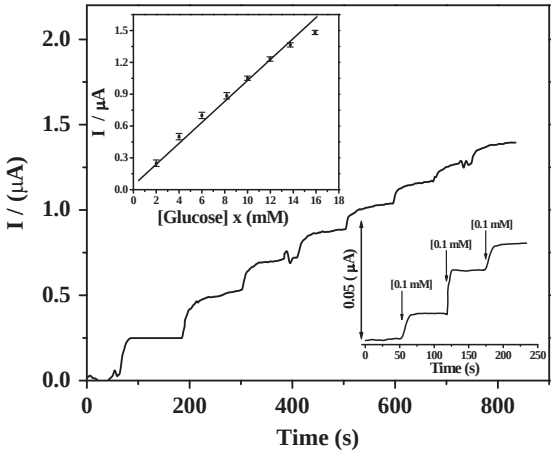

Fig. 5. The amperometric response of biosensor at 0.4 V upon successive additions of glucose in air-saturated 10 mmol L^{-1} PBS (pH 6.0). Inset upper: amperometric response curve for glucose. Inset lower: amperometric response after successive additions of 0.1 mmol L^{-1} glucose.

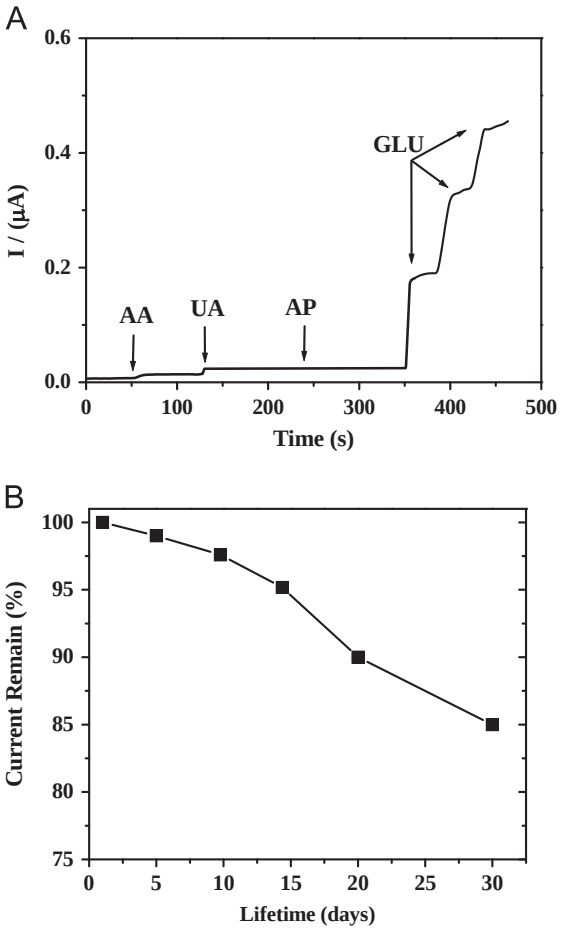

Fig. 6. (A) Chronoamperometric response to the injection 0.5 mmol L^{-1} ascorbic acid (AA), 0.5 mmol L^{-1} uric acid (UA), 0.5 mmol L^{-1} acetoaminophen common interferences, and 0.5 mmol L^{-1} glucose. The applied potential was 0.4 V. (B) The operational stability of biosensor at different day period.

was not in use, it was stored in buffer at 4 °C. The current response decreases slightly in the first few days, and afterward, the response tends to be practically constant and retained 85% of its original response over two months of storage. However, because of the kinetic mode operation, this biosensor can be easily calibrated during all operational time, and significant reduction of the initial activity is not a problem as far as the slope of calibration curve is sufficiently steep to provide appropriate sensor parameters and reliable detection. The RSD is 4.2% estimated from slopes of calibration plots of freshly prepared electrodes, revealing an acceptable repeatability.

3.7. Determination of glucose in serum

Human serum samples were assayed to show the practical utility of this glucose biosensor. Serum samples and glucose concentrations were provided by a local hospital biochemistry laboratory. Results were compared with those determined by local university hospital using colorimetric method with glucose kit (Boehringer enzyme kit). The results closely agree with those values measured in the hospital (Table 1). The *t*-value was found as 0.393 at 95% confidence level. The results obtain agreement between the two methods, which allow the development of biosensor suitability to practical applications at confidence level of 95%.

Table 1
Determination of blood glucose in human serum samples.

Concentration of glucose (mmol L^{-1})		
Samples	**Biosensor**	**Glucose assay kit**
1	6.0 ± 0.5	6.2 ± 0.4
2	6.1 ± 0.6	6.0 ± 0.3
3	6.3 ± 0.4	6.4 ± 0.4
4	6.1 ± 0.3	5.9 ± 0.2

4. Conclusion

In summary, we have successfully constructed a glucose biosensor by dropping multisegments nanowires onto the surface of a GC. The obtained results have demonstrated the possibility of magnetoswitchable over bioelectrocatalytic transformations through reorientation of nanowires. The resulting biosensor exhibited good amperometric response to glucose in PBS and human blood serum. It also presented a number of other attractive features such as fast response, long-term storage stability, high reproducibility, and satisfactory anti-interference ability. The multisegment nanowires developed here offer a new approach for constructing novel biosensors and can provide a new way to control bioelectrocatalysis by magnetic control.

Acknowledgments

The authors thank FAPESP (2010/07478-5), Coordenação de Aperfeiçoamento de Pessoal de Nível Superior (CAPES) and CNPq (475871/2011-1), Brazil, for the grants and the financial support to this work.

References

[1] R. Devi, C.S. Pundir, Sens. Actuators B 193 (2014) 608–615.
[2] M. Wooten, S. Karra, M.G. Zhang, W. Gorski, Anal. Chem. 86 (2014) 752–757.
[3] S. Mantha, V.A. Pedrosa, E.V. Olsen, V.A. Davis, A.L. Simonian, Langmuir 26 (2010) 19114–19119.
[4] E. Koposova, X. Liu, A. Kisner, Y. Ermolenko, G. Shumilova, A. Offenhäusser, Y. Mourzina, Biosens. Bioelectron. 57 (2014) 54–58.
[5] L.C. Recco, I. Tokarev, S. Minko, V.A. Pedrosa, Chem. Eur. J. 20 (2014) 1226–1230.
[6] P. Rosa, M. Linda, V. Angelo, TrAc Trends Anal. Chem. 47 (2013) 12–26.
[7] S.J. Guo, D. Wen, S.J. Dong, E.K. Wang, Talanta 77 (2009) 1510–1517.
[8] X. Kang, Z. Mai, X. Zou, P. Cai, J. Mo, Anal. Biochem. (2007) 143–150.
[9] B.K. Jena, C.R. Raj, Anal. Chem. 78 (2006) 6332–6339.
[10] C. Yang, C. Xu, X. Wang, Langmuir 28 (2012) 4580–4585.
[11] J. Xu, F. Shang, J.H.T. Luong, K.M. Razeeb, J.D. Glennon, Biosens. Bioelectron. 25 (2010) 1313–1318.
[12] J. Wang, Analyst 130 (2005) 421–426.
[13] Masato Saito Kagan Kerman, Eiichi Tamiya, Shohei Yamamura, Yuzuru Takamura, TrAC Trends Anal. Chem. 27 (2008) 585–592.
[14] Y. Chen, Y. Luo, Adv. Mater. 21 (2009) 2040–2044.
[15] K.M. Byun, S.J. Yoon, D. Kim, S.J. Kim, Opt. Lett. 32 (2007) 1902–1904.
[16] A.K. Wanekaya, W. Chen, N.V. Myung, A. Mulchandani, Electroanalysis 18 (2006) 533–555.
[17] X. Liu, P. Lin, X. Yan, Z. Kang, Y. Zhao, Y. Lei, C. Li, H. Du, Y. Zhang, Sens. Actuators B 216 (2013) 22–27.
[18] Q. Wang, F. Min., J. Zhu, Mater. Lett. 91 (2013) 9–11.
[19] Z.H. Ibupoto, H. Jamal, K. Khun, M. Willander, Sens. Actuators B 166 (2012) 809–814.
[20] J. Wang, M. Scampicchio, R. Laocharoensuk, F. Valentini, O.G. García, J. Burdick, J. Am. Chem. Soc. 128 (2006) 4562–4563.
[21] K.M. Leung, G. Wanger, M.Y. El-Naggar, Y. Gorby, G. Southam, W.M. Lau, J. Yang, Nano Lett. 13 (2013) 2407–2411.
[22] M. García, J.R.A. Fernández, A. Escarpa, Anal. Chem. 85 (2013) 9116–9125.
[23] J. Wang, Chem. Phys. Chem. 10 (2009) 1748–1755.
[24] Y. Yang, L. Lin, Y. Zhang, Q. Jing, T.C. Hou, Z.L. Wang, ACS Nano 6 (2012) 10378–10383.
[25] V.A. Pedrosa, X. Luo, J. Burdick, J. Wang, Small 4 (2008) 738–741.
[26] O.A. Loioza, R. Laocharoensuk, J. Burdick, M.C. Rodriguez, J.M. Pingarron, M. Pedrero, J. Wang, Angew. Chem. 119 (2007) 1530–1533.
[27] M.F. Cabral, M.L. Calegaro, S.A.S. Machado, RSC Adv. 2 (2012) 2498–2503.
[28] Y. Mu, D. Jia, Y. He, Y. Miao, H.L. Wu, Biosens. Bioelectron. 26 (2011) 2948–2952.
[29] M. Shamsipur, M. Najafi, M.R.M. Hosseini, Bioelectrochemistry 77 (2010) 120–124.
[30] L. Zheng, J.Q. Zhang, J.F. Song, Electrochim. Acta 54 (2009) 4559–4565.
[31] X. Chen, J. Chen, C. Deng, C. Xiao, Y. Yang, Z. Nie, S. Yao, Talanta 76 (2008) 763–767.